Letter

Uncovering measurement-induced entanglement via directional adaptive dynamics and incomplete information

Yu-Xin Wang (王语馨),[1,2,*] Alireza Seif,[1] and Aashish A. Clerk[1]

[1]*Pritzker School of Molecular Engineering, University of Chicago, Chicago, Illinois 60637, USA*

[2]*Joint Center for Quantum Information and Computer Science, University of Maryland, College Park, Maryland 20742, USA*

(Received 17 October 2023; revised 19 August 2024; accepted 29 October 2024; published 19 November 2024)

The rich entanglement dynamics and transitions exhibited by monitored quantum systems typically only exist in the conditional state, making observation extremely difficult. In this Letter, we construct a general recipe for mimicking the conditional entanglement dynamics of a monitored system in a corresponding measurement-free dissipative system involving directional interactions between the original system and a set of auxiliary register modes. This mirror setup autonomously implements a measurement-feedforward dynamics that effectively retains a coarse-grained measurement record. We illustrate our ideas in a bosonic system featuring a competition between entangling measurements and local unitary dynamics, and also discuss extensions to qubit systems and truly many-body systems.

DOI: 10.1103/PhysRevA.110.L050602

Introduction. Entanglement is a unique feature of quantum systems, and studying its dynamics in complex systems has both fundamental and practical motivations. To wit, there is immense interest in understanding different phases of entanglement generation in systems having a competition between Hamiltonian and measurement-induced dynamics (see, e.g., Refs. [1–16]). A common feature here is that entanglement generation is contingent on knowing the measurement results, i.e., it only exists at the level of individual measurement trajectories [see Fig. 1(a)]. Conversely, the average state (averaged over all measurement outcomes) is typically highly mixed and unentangled. As such, direct detection of novel entanglement dynamics and transitions would seem to require postselection over measurement records, posing formidable challenges for scalable experimental implementation [17].

Various ideas have been suggested to tackle this postselection problem [18–29], with some corresponding experimental implementations [30,31]. Many of these approaches focus on measuring a proxy quantity (i.e., not system entanglement directly), or study a transition in the efficiency of using feedback-assisted dynamics to stabilize a preselected target state [with this transition serving as a proxy for the actual measurement-induced entanglement phase transitions (MIPT) of interest [23–26]]. While those approaches do not require postselection, one might worry that the transitions in feedback-assisted dynamics might be distinct and only loosely related to the original entanglement phase transition [25–27,32–35].

Given this, it would be highly desirable to have a fully deterministic, postselection-free protocol whose entanglement dynamics (and not some proxy quantity) quantitatively reproduces transitions in the trajectory-level entanglement of a measured system. In this Letter, we introduce such a strategy. We start with a system of interest, where a combination of Hamiltonian dynamics and continuous measurements leads to interesting features in the *postselected* entanglement dynamics [Fig. 1(a)]. To access this physics, we propose studying a distinct, modified setup that includes the original system (the "target") and its Hamiltonian dynamics. We now have no explicit measurements, but instead introduce one or more "register" systems, and implement *dissipative* dynamics that *directionally* couples the target to these registers. This dissipative dynamics is constructed to autonomously mimic an adaptive process involving continuous measurement on the target, followed by conditional feedforward driving of the register [36–38] [Fig. 1(b)].

Unlike protocols based on deferred measurement [30,32], our setup does not generate any entanglement between the register and the system. Further, it only retains a vanishingly small fraction of the information that would be contained in an actual measurement record. Despite these caveats, we find that if one considers an appropriate bipartition (where part of the target is grouped with the registers), the entanglement of the constructed dissipative dynamics can quantitatively capture features of entanglement generation in the original monitored, postselected system. Our approach thus has the potential of providing a new and powerful method for accessing MIPTs.

While our scheme is general, we focus here on a relatively unexplored setting, where there is a competition between collective entanglement-generating measurements and a set of local Hamiltonians that can either enhance or suppress entanglement creation. This is the opposite of what is typically studied, where the focus is instead on the interplay between entangling unitaries and competing measurements [1–13].

*Contact author: yxwang@uchicago.edu

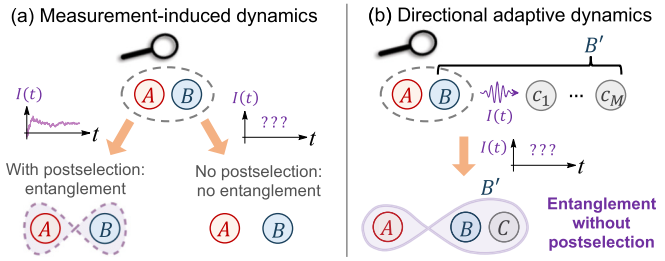

FIG. 1. Adaptive approach for mimicking entanglement dynamics of a monitored system. (a) A collective measurement creates conditional entanglement between A and B, whereas the unconditional state (averaged over measurement outcomes) is unentangled. (b) By applying a conditional feedforward operation on auxiliary register modes c_j $(j = 1, 2, \ldots, M)$, partial information from the measurement record is retained. This can be enough to maintain entanglement in the unconditional state [now between A and the composite subsystem of (B, c_j)]. This dynamics can be realized fully autonomously (without any measurement) using an engineered dissipative process [cf. Eq. (3)].

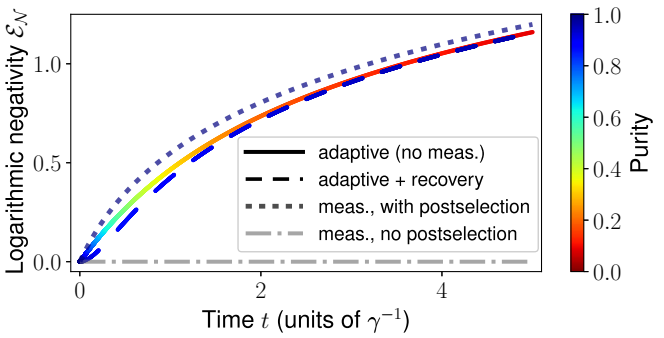

FIG. 2. Preservation of postselected entanglement generation via adaptive dynamics. Dotted curve: Conditioned entanglement growth between modes a and b, quantified by logarithmic negativity $\mathcal{E}_\mathcal{N}^{(\mathrm{ps})}$, of the postselected state generated by continuous measurement of the quadrature $\hat{x}_+ \equiv (\hat{x}_a + \hat{x}_b)/\sqrt{2}$ [see Eq. (2)]. Solid and dashed curves: Deterministic entanglement between modes a and (b, c) as generated by the postselection-free dissipative dynamics in Eq. (4), for cases with (solid curve) and without (dashed curve) recovery via projection measurement of mode c quadrature $\hat{\pi}$ and conditional feedback. Coloring of the curves (except gray) corresponds to state purity. Parameter: $\eta = 1$.

Our adaptive-dynamics setup generates entanglement growth that exhibits almost the same parametric dependence as the original measured, postselected system. As an application, we show that for two bosonic modes, the adaptive dynamics generates unlimited entanglement with logarithmic growth in time. We also show that our measurement-free approach to realizing MIPTs is directly applicable to many-body settings, as well as nonlinear systems such as qubits and qudits. We end by discussing experimental implementations, which are within reach using current physical platforms.

Basic setup. While our scheme is suitable for many-body systems, to illustrate the basic ideas we start by analyzing the simplest nontrivial example: a target system consisting of two bosonic modes, a and b. We define quadrature operators in terms of annihilation operators $\hat{a}$ and $\hat{b}$ as $\hat{x}_m \equiv (\hat{m} + \hat{m}^\dagger)/\sqrt{2}$ $(m = a, b)$. Consider the postselected dynamics due to competing processes of a continuous entangling measurement of the collective quadrature $\hat{x}_+ \equiv (\hat{x}_a + \hat{x}_b)/\sqrt{2}$, and a local Hamiltonian

$$\hat{H}_{\mathrm{det}} = (\omega + \delta\omega)\hat{a}^\dagger\hat{a} + (-\omega + \delta\omega)\hat{b}^\dagger\hat{b}. \tag{1}$$

It is well known that large many-body lattice systems can exhibit distinct phases of entanglement dynamics, characterized by entanglement either growing linearly or logarithmically in time (volume law or critical phases), or saturating (area law phases). Similar regimes can also exist in few mode bosonic systems, something that is enabled by their infinite-dimensional Hilbert space. We find that depending on parameters, the measurement-induced, intermode entanglement generation in the two-mode system above can exhibit drastically different asymptotic regimes, due to a competition between the entangling measurement and nonentangling Hamiltonian dynamics.

To quantify entanglement, we will use the logarithmic negativity $\mathcal{E}_\mathcal{N}^{(\mathrm{ps})}$ of the postselected state. In the absence of a Hamiltonian $(\omega = \delta\omega = 0)$ and for an initial vacuum state, we obtain unbounded entanglement growth (see Fig. 2)

$$\mathcal{E}_\mathcal{N}^{(\mathrm{ps})} = (1/2)\ln(1 + 2\gamma t), \tag{2}$$

where γ and t denote measurement rate and evolution time, respectively [39] (see Supplemental Material [40] for details). The logarithmic temporal dependence of entanglement generation is known to be a feature of conformal invariance [41], and emerges in nonequilibrium systems including many-body localized phases [42–44] and measurement-induced dynamics [45,46]. Here, the logarithmic scaling arises due to quantum-nondemolition (QND) measurement-induced squeezing (see Ref. [47] for a Hamiltonian version of this effect).

If we now include local Hamiltonian dynamics generated by Eq. (1), we find that entanglement growth is hindered whenever $\delta\omega \neq 0$: There is no longer any unbounded growth. In contrast (and somewhat surprisingly), the local Hamiltonian dynamics can *enhance* entanglement generation when $\delta\omega = 0$ and ω is nonzero. We stress these different regimes of entanglement dynamics can only be seen with postselection: If one instead averages over all the measurement outcomes, the resulting unconditioned state is unentangled at all times (irrespective of parameters).

We now seek to reproduce the conditional entanglement dynamics of this measured system in a second postselection-free (and potentially measurement-free) setup. Making use of the general recipe laid out in the introduction, we consider an adaptive process where a coarse-grained version of the measurement record obtained from monitoring $\hat{x}_+$ is retained in a set of auxiliary register bosonic modes c_j $(j = 1, 2, \ldots, M)$. This could be achieved by partitioning the total evolution time t_f into M equal intervals, and in each interval, using the measurement record to linearly force one of the M register modes [see Fig. 1(b)]. As shown in Refs. [36–38], the *unconditioned* evolution from such a process in the zero-delay limit is described by the master equation

$$(d\hat{\rho}/dt) = -i[\hat{H}_{\mathrm{det}}, \hat{\rho}] + \gamma \sum_{j=1}^{M} f_j(t; t_f)\mathcal{L}_{\hat{x}_+ \to \eta\hat{y}_j}\hat{\rho}, \tag{3}$$

where $f_j(t;t_f) \equiv \Theta(t - \frac{j-1}{M}t_f)\Theta(\frac{j}{M}t_f - t)$ ensures the measurement record from the jth interval drives the register mode $\hat{c}_j$ [$\Theta(\cdot)$ is the Heaviside step function]. We define the Lindbladians $\mathcal{L}_{\hat{x}_+\to\eta\hat{y}_j}$ as

$$\mathcal{L}_{\hat{x}_+\to\eta\hat{y}_j}\hat{\rho} \equiv -i[\eta\hat{x}_+\hat{y}_j, \hat{\rho}] + \mathcal{D}[\hat{x}_+ - i\eta\hat{y}_j]\hat{\rho}, \tag{4}$$

with $\hat{y}_j \equiv (\hat{c}_j + \hat{c}_j^\dagger)/\sqrt{2}$ a quadrature of register j, η a constant quantifying feedforward strength, and $\mathcal{D}[\hat{O}]\hat{\rho} \equiv (\hat{O}\hat{\rho}\hat{O}^\dagger - \{\hat{O}^\dagger\hat{O}, \hat{\rho}\}/2)$ denoting the standard Lindblad dissipator [48,49].

While we have motivated Eq. (4) by considering unconditional evolution in a setup with explicit measurements and feedforward, identical dynamics could be achieved without any measurements at all: One could engineer an autonomous dissipative process that yields the same master equation (using the tools of reservoir engineering; see, e.g., Ref. [50]). This then provides a potential measurement-free route for probing the entanglement physics of the original monitored system. We stress that the system-only dynamics is completely unaffected by the feedforward step, i.e., if we trace out the auxiliary registers in Eq. (3), the system dynamics faithfully recovers the unconditioned evolution associated with measuring $\hat{x}_+$. This is in marked contrast to schemes employing feedback-assisted dynamics [23–26].

We first consider our scheme in the simple case $\hat{H}_{\rm det} = 0$. Surprisingly, we find that using a single register mode c [i.e., setting $M = 1$ in Eq. (3)] is sufficient to capture the desired entanglement dynamics. This can be seen by computing the entanglement of the total system state, with the bipartition between modes a vs (b, c). As shown in Fig. 2, in the long-time limit $\gamma t \gg 1$, the unconditioned state generated by the dissipative dynamics in Eq. (3) with $\eta = 1$ and all the modes in initial vacuum states (solid curve) fully preserves the conditioned entanglement just from measuring $\hat{x}_+$ (dotted curve). We also provide analytic arguments in the Supplemental Material [40] for why a single register mode is sufficient in this case, and show that the entanglement of formation $\mathcal{E}_F$ has similar dynamics to the log negativity. While we took the relative feedforward strength $\eta = 1$ here, using larger values always enhances our scheme's ability to capture entanglement, as it makes one less sensitive to quantum noise in the initial register state [40]. We will nonetheless focus throughout on modest η values, as this is sufficient for good performance and much more compatible with experiment.

While Eq. (3) generates entanglement that closely mimics the conditional dynamics of the original monitored system, it does not generate a pure state; in fact, the purity decreases with time (see Supplemental Material [40] for an analogous effect in a qubit system). Using the measurement-feedforward interpretation of Eq. (3), this can be attributed to the random nature of a given measurement trajectory. Fortunately, as shown in the dashed curves in Fig. 2, one can still recover almost pure-state entanglement from this highly mixed state via a single Gaussian, projection measurement on mode c, followed by local, conditional feedback operations on the target modes (see Supplemental Material [40]).

Capturing nontrivial entanglement features. We return to Eq. (3), and now consider dynamics with both collective measurement and a competing local Hamiltonian. Consider first

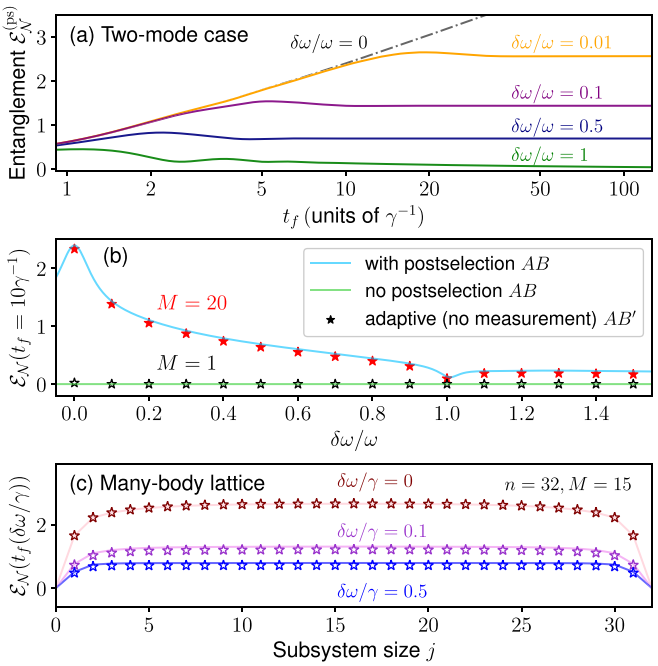

FIG. 3. (a) Time-dependent (a, b) entanglement in the postselected state generated from the combination of Hamiltonian dynamics as per Eq. (1) and continuous measurement of $\hat{x}_+$. (b) Light blue: Measurement-induced entanglement at a fixed evolution time $t_f = 10\gamma^{-1}$, as a function of the Hamiltonian parameter $\delta\omega$. Red asterisks: Same, but entanglement generated by our measurement-free adaptive-dynamics scheme with $M = 20$ registers [see Eq. (3)], with respect to the bipartition between a and the rest of the system. The adaptive scheme quantitatively captures the nontrivial parameter dependence of the conditional entanglement generated in the original measured setup. Parameters in (a) and (b): $\omega/\gamma = 1.2$, $\eta = 5$, $t_f = 10\gamma^{-1}$. (c) Solid lines: Entanglement page curve (between the first j sites and the rest of the system) generated by conditional dynamics under uniform on-site detunings ($\delta\omega \neq 0$) and measurements on nearest-neighbor bonds (with strength γ) on a 32-site lattice. Asterisks: Entanglement created via the corresponding measurement-free adaptive protocol [see Eq. (3)]. Parameters: $M = 15$, $\eta = 5$. Total protocol time is chosen as $t_f = 50\gamma^{-1}$ for $\delta\omega = 0$, or the time when entanglement stabilizes in the conditional dynamics or the measurement-free adaptive protocol, respectively (see Supplemental Material [40] for details).

features of the measured dynamics with postselection, which as mentioned can exhibit unbounded entanglement growth ($\delta\omega = 0$) or saturation ($\delta\omega \neq 0$) in the long-time limit, as shown in Fig. 3(a). Surprisingly, adding a local Hamiltonian can enhance long-time entanglement growth [logarithmic growth that is twice as fast compared to Eq. (2)] when $\delta\omega = 0$ and $\omega \neq 0$. As shown in the Supplemental Material [40], this can be understood via a special symmetry structure of $\hat{H}_{\rm det}$, often termed a quantum-mechanics-free subsystem (QMFS) [51,52]. If the system is weakly perturbed by tuning $\delta\omega$ away from the QMFS parameter point, the logarithmic negativity at a fixed evolution time exhibits a sharp peak at $\delta\omega = 0$ [see the light blue curve in Fig. 3(b)]. The entanglement of the conditional state also shows curious nonmonotonic-in-time features when the perturbation crosses the point $\delta\omega = \omega$ [cf.

the green curve in Fig. 3(a)]; at that specific parameter choice, the entanglement vanishes in the asymptotic long-time limit.

We now come to a central result of this Letter: The nontrivial features in the postselected entanglement generation discussed above can be faithfully captured in the *unconditional* state produced by the dissipative dynamics of Eq. (3) [see Fig. 1(b)]. We plot in Fig. 3(b) the entanglement generated between a (subsystem A) and the expanded system of b and M register modes (subsystem B') as a function of $\delta\omega$ [obtained numerically from Eq. (3)]. Using $M = 20$ register modes (corresponding to a coarse-graining timescale $\Delta t \sim t_f/20 = 0.5\gamma^{-1}$) allows us to closely reproduce the postselected entanglement dynamics, even though this retains a tiny fraction of the full measurement records [53] (see Supplemental Material [40] for more details).

Generalizations. The adaptive-dynamics approach can be generalized to a variety of more complex systems. As a many-body extension of our bosonic example, we consider a one-dimensional (1D) bosonic lattice subject to continuously monitoring of linear bond variables. Such dynamics can create long-range entanglement in the conditional state and host measurement-induced entanglement transitions [13,14]. Further, the conditional entanglement transitions from log law ($\delta\omega = 0$) to area law ($\delta\omega \neq 0$) in the presence of an on-site Hamiltonian, $\hat{H}_{\text{det,multi}} = \delta\omega \sum_{j=1}^{n} \hat{a}_j^\dagger \hat{a}_j$. As shown in Fig. 3(c), a direct multimode generalization of the autonomous protocol in Eq. (3) lets us capture conditional entanglement generation in the two regimes without any measurement or postselection (see Supplemental Material [40] for simulation details). Importantly, the coarse-graining procedure as per Eq. (3) quantitatively preserves the spatial entanglement structure using values of the feedforward parameter ($\eta = 5$) and the number of registers per bond ($M = 15$) that are comparable to the two-mode case. Further simulations with varying system sizes [40] show that for our protocol to quantitatively reproduce the conditional entanglement generation, the required M and η do not scale with n, indicating that our protocol generalizes to many-body systems with a hardware overhead scaling linearly in system size.

It is also worth noting that the bosonic systems discussed thus far can be directly mapped to genuinely many-body qubit systems, where each bosonic mode becomes an ensemble of $2S$ spins ($S \gg 1$) and the quadrature operator $\hat{x}_a$ is replaced with the rescaled total angular momentum operator of the ath ensemble along the x axis, $\hat{x}_a \to \hat{S}_{a,x}/\sqrt{S}$, via the Holstein-Primakoff transformation [54]. The aforementioned bosonic 1D system can thus describe an array of spin ensembles with nontrivial connectivity; such systems with programmable connectivity have been recently realized experimentally using atomic ensembles (see, e.g., Refs. [55,56]).

Another generalization is to move beyond quadratic bosonic systems. This immediately creates extra complexity, as now measurement-induced entanglement in the postselected state can fluctuate from trajectory to trajectory [57]. Despite this, for several examples in this more general category, we find that our adaptive scheme still provides a means for replicating conditional measurement-induced entanglement. For concreteness, consider a target system of two qubits undergoing a continuous measurement of a nonlocal operator $\hat{\Sigma}_x$. For our autonomous scheme, we will use

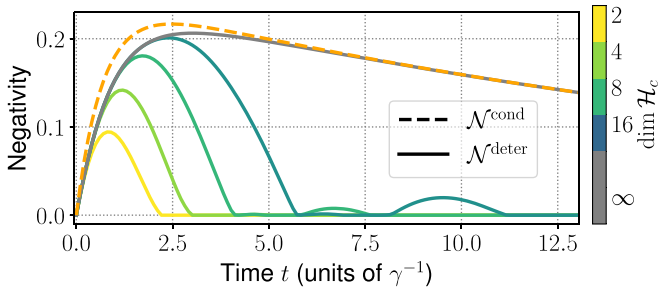

FIG. 4. Deterministic entanglement generation between qubit 1 and extended systems consisting of qubit 2 and an auxiliary d-dimensional register c, via the adaptive dynamics in Eq. (5) that realize an autonomous measurement-and-feedforward process (solid curves). In the asymptotic long-time limit and for c being a bosonic mode with a quadrature as the feedforward operator, the deterministic entanglement (gray solid curve) perfectly replicates the trajectory-averaged conditioned entanglement (black dashed curve) created by a weak nonlocal measurement of $\hat{\Sigma}_x \equiv (\hat{\sigma}_{x,1} + 0.7\hat{\sigma}_{x,2})/2$ at intermediate and large timescales. Parameter: $\eta = 1$.

a single d-dimensional auxiliary register system, yielding a dynamics

$$(d\hat{\rho}/\gamma dt) = -i[\eta\hat{\Sigma}_x\hat{F}, \hat{\rho}] + \mathcal{D}[\hat{\Sigma}_x - i\eta\hat{F}]\hat{\rho}, \tag{5}$$

where $\eta, \hat{F}$ denote the feedforward strength and feedforward operator acting on the register, respectively. We take $\hat{\Sigma}_x \equiv (\hat{\sigma}_{x,1} + 0.7\hat{\sigma}_{x,2})/2$ and $\hat{F}$ a truncated bosonic quadrature operator acting on the auxiliary qudit (note the applicability of our protocol does not rely on specific form of these operators, see Supplemental Material [40]). As shown in Fig. 4, the measurement-free dynamics in Eq. (5) accurately captures features of the conditioned entanglement at short to moderate times. At longer times there is no longer a correspondence, something that is simply understood as being the result of the finite dimensionality of the register (e.g., there is no longer sufficient dynamic range to store measurement outcomes). Increasing the dimension of the register $d \equiv \dim \mathcal{H}_c$ (see Fig. 4) increases the effective dynamic range of the register, thus enhancing its ability to store information.

Discussions. We have presented a general measurement-free method for replicating conditional entanglement generated in a continuously monitored system. It involves engineering directional interactions with an auxiliary register system which effectively retains a small fraction of the information content in a given measurement record. The examples we consider suggest that despite the seemingly large loss of information contained in the specific measurement outcomes, this approach can quantitatively capture entanglement features arising from the competition between measurements and unitary dynamics, as measured by negativity-based quantities. In future work, it would be interesting to understand more rigorously the question of how much of the measurement record in a generic setup can be discarded before our scheme breaks down. While our work focused on logarithmic negativity, another question worth further exploration is whether one can recover more general entanglement measures, such as higher Rényi entanglement entropies, via our measurement-free protocol.

We note that the key ingredients of our scheme can be realized either directly in physical platforms that inherently allow nonreciprocal QND interactions, e.g., in levitated nanoparticles [58], or synthetically using standard reservoir engineering techniques [59,60]; the latter has been demonstrated in a variety of experimental platforms [61–66] (see Supplemental Material [40] for details).

Our work ultimately employs feedforward dynamics, and hence connects to other general topics in quantum dynamics. This includes ideas for how feedback and feedforword can enhance the power of shallow quantum circuits [67–69]. It also connects to the question of if and when dissipative Markovian dephasing dynamics can create entanglement, an issue that can also be mapped to effective feedforward processes [70]. Our results here provide an intuitive understanding of how entanglement can be generated by such correlated dephasing processes (see Supplemental Material [40]).

Acknowledgments. We thank Marko Cetina, Liang Jiang, and Michael Gullans for useful discussions. This work was supported by the Air Force Office of Scientific Research under Grant No. FA9550-19-1-0362. A.C. also acknowledges support from the Simons Foundation through a Simons Investigator Award (Grant No. 669487, A.C.).

[1] B. Skinner, J. Ruhman, and A. Nahum, Measurement-induced phase transitions in the dynamics of entanglement, Phys. Rev. X **9**, 031009 (2019).

[2] Y. Li, X. Chen, and M. P. A. Fisher, Measurement-driven entanglement transition in hybrid quantum circuits, Phys. Rev. B **100**, 134306 (2019).

[3] A. Zabalo, M. J. Gullans, J. H. Wilson, S. Gopalakrishnan, D. A. Huse, and J. H. Pixley, Critical properties of the measurement-induced transition in random quantum circuits, Phys. Rev. B **101**, 060301(R) (2020).

[4] Y. Bao, S. Choi, and E. Altman, Theory of the phase transition in random unitary circuits with measurements, Phys. Rev. B **101**, 104301 (2020).

[5] S. Choi, Y. Bao, X.-L. Qi, and E. Altman, Quantum error correction in scrambling dynamics and measurement-induced phase transition, Phys. Rev. Lett. **125**, 030505 (2020).

[6] A. Lavasani, Y. Alavirad, and M. Barkeshli, Measurement-induced topological entanglement transitions in symmetric random quantum circuits, Nat. Phys. **17**, 342 (2021).

[7] X. Turkeshi, A. Biella, R. Fazio, M. Dalmonte, and M. Schiró, Measurement-induced entanglement transitions in the quantum Ising chain: From infinite to zero clicks, Phys. Rev. B **103**, 224210 (2021).

[8] M. Van Regemortel, Z.-P. Cian, A. Seif, H. Dehghani, and M. Hafezi, Entanglement entropy scaling transition under competing monitoring protocols, Phys. Rev. Lett. **126**, 123604 (2021).

[9] O. Alberton, M. Buchhold, and S. Diehl, Entanglement transition in a monitored free-fermion chain: From extended criticality to area law, Phys. Rev. Lett. **126**, 170602 (2021).

[10] T. Botzung, S. Diehl, and M. Müller, Engineered dissipation induced entanglement transition in quantum spin chains: From logarithmic growth to area law, Phys. Rev. B **104**, 184422 (2021).

[11] A. Lavasani, Y. Alavirad, and M. Barkeshli, Topological order and criticality in $(2+1)$D monitored random quantum circuits, Phys. Rev. Lett. **127**, 235701 (2021).

[12] P. M. Poggi and M. H. Muñoz-Arias, Measurement-induced multipartite-entanglement regimes in collective spin systems, Quantum **8**, 1229 (2024).

[13] Y. Minoguchi, P. Rabl, and M. Buchhold, Continuous Gaussian measurements of the free boson CFT: A model for exactly solvable and detectable measurement-induced dynamics, SciPost Phys. **12**, 009 (2022).

[14] K. Yokomizo and Y. Ashida, Measurement-induced phase transition in free bosons, arXiv:2405.19768.

[15] A. C. Potter and R. Vasseur, Entanglement dynamics in hybrid quantum circuits, in *Quantum Science and Technology* (Springer, Cham, 2022), pp. 211–249.

[16] M. P. Fisher, V. Khemani, A. Nahum, and S. Vijay, Random quantum circuits, Annu. Rev. Condens. Matter Phys. **14**, 335 (2023).

[17] J. M. Koh, S.-N. Sun, M. Motta, and A. J. Minnich, Measurement-induced entanglement phase transition on a superconducting quantum processor with mid-circuit readout, Nat. Phys. **19**, 1314 (2023).

[18] M. Ippoliti and V. Khemani, Postselection-free entanglement dynamics via spacetime duality, Phys. Rev. Lett. **126**, 060501 (2021).

[19] A. G. Moghaddam, K. Pöyhönen, and T. Ojanen, Exponential shortcut to measurement-induced entanglement phase transitions, Phys. Rev. Lett. **131**, 020401 (2023).

[20] H. Dehghani, A. Lavasani, M. Hafezi, and M. J. Gullans, Neural-network decoders for measurement induced phase transitions, Nat. Commun. **14**, 2918 (2023).

[21] S. J. Garratt and E. Altman, Probing postmeasurement entanglement without postselection, PRX Quantum **5**, 030311 (2024).

[22] G. Passarelli, X. Turkeshi, A. Russomanno, P. Lucignano, M. Schiró, and R. Fazio, Many-body dynamics in monitored atomic gases without postselection barrier, Phys. Rev. Lett. **132**, 163401 (2024).

[23] T. Iadecola, S. Ganeshan, J. H. Pixley, and J. H. Wilson, Measurement and feedback driven entanglement transition in the probabilistic control of chaos, Phys. Rev. Lett. **131**, 060403 (2023).

[24] M. Buchhold, T. Müller, and S. Diehl, Revealing measurement-induced phase transitions by pre-selection, arXiv:2208.10506.

[25] P. Sierant and X. Turkeshi, Controlling entanglement at absorbing state phase transitions in random circuits, Phys. Rev. Lett. **130**, 120402 (2023).

[26] N. O'Dea, A. Morningstar, S. Gopalakrishnan, and V. Khemani, Entanglement and absorbing-state transitions in interactive quantum dynamics, Phys. Rev. B **109**, L020304 (2024).

[27] P. Sierant and X. Turkeshi, Entanglement and absorbing state transitions in $(d+1)$-dimensional stabilizer circuits, Acta Phys. Pol., A **144**, 474 (2023).

[28] M. J. Gullans and D. A. Huse, Scalable probes of measurement-induced criticality, Phys. Rev. Lett. **125**, 070606 (2020).

[29] Y. Li, Y. Zou, P. Glorioso, E. Altman, and M. P. A. Fisher, Cross entropy benchmark for measurement-induced phase transitions, Phys. Rev. Lett. **130**, 220404 (2023).

[30] C. Noel, P. Niroula, D. Zhu, A. Risinger, L. Egan, D. Biswas, M. Cetina, A. V. Gorshkov, M. J. Gullans, D. A. Huse, and C. Monroe, Measurement-induced quantum phases realized in a trapped-ion quantum computer, Nat. Phys. **18**, 760 (2022).

[31] J. C. Hoke, M. Ippoliti, D. Abanin, R. Acharya, M. Ansmann, F. Arute, K. Arya, A. Asfaw, J. Atalaya, J. C. Bardin *et al.*, Measurement-induced entanglement and teleportation on a noisy quantum processor, Nature (London) **622**, 481 (2023).

[32] A. J. Friedman, O. Hart, and R. Nandkishore, Measurement-induced phases of matter require feedback, PRX Quantum **4**, 040309 (2023).

[33] L. Piroli, Y. Li, R. Vasseur, and A. Nahum, Triviality of quantum trajectories close to a directed percolation transition, Phys. Rev. B **107**, 224303 (2023).

[34] V. Ravindranath, Z.-C. Yang, and X. Chen, Free fermions under adaptive quantum dynamics, arXiv:2306.16595.

[35] C. LeMaire, A. A. Allocca, J. H. Pixley, T. Iadecola, and J. H. Wilson, Separate measurement- and feedback-driven entanglement transitions in the stochastic control of chaos, Phys. Rev. B **110**, 014310 (2024).

[36] H. M. Wiseman, Quantum theory of continuous feedback, Phys. Rev. A **49**, 2133 (1994).

[37] H. M. Wiseman and G. J. Milburn, *Quantum Measurement and Control* (Cambridge University Press, Cambridge, UK, 2009).

[38] A. Metelmann and A. A. Clerk, Nonreciprocal quantum interactions and devices via autonomous feedforward, Phys. Rev. A **95**, 013837 (2017).

[39] In this specific case, as the dynamics is Gaussian, every trajectory has the same entanglement.

[40] See Supplemental Material at http://link.aps.org/supplemental/10.1103/PhysRevA.110.L050602 for details on trajectory dynamics due to continuously monitoring $\hat{x}_+$, parametric dependence of conditional entanglement generation and entanglement via the corresponding measurement-free protocol, the recovery protocol, and the reservoir engineering realization of each dissipator in Eq. (3), which includes Refs. [71–76].

[41] P. Calabrese and J. Cardy, Entanglement entropy and quantum field theory, J. Stat. Mech.: Theory Exp. (2004) P06002.

[42] M. Žnidarič, T. Prosen, and P. Prelovšek, Many-body localization in the Heisenberg XXZ magnet in a random field, Phys. Rev. B **77**, 064426 (2008).

[43] J. H. Bardarson, F. Pollmann, and J. E. Moore, Unbounded growth of entanglement in models of many-body localization, Phys. Rev. Lett. **109**, 017202 (2012).

[44] D. A. Abanin, E. Altman, I. Bloch, and M. Serbyn, Colloquium: Many-body localization, thermalization, and entanglement, Rev. Mod. Phys. **91**, 021001 (2019).

[45] C.-M. Jian, Y.-Z. You, R. Vasseur, and A. W. W. Ludwig, Measurement-induced criticality in random quantum circuits, Phys. Rev. B **101**, 104302 (2020).

[46] Y. Li, X. Chen, A. W. W. Ludwig, and M. P. A. Fisher, Conformal invariance and quantum nonlocality in critical hybrid circuits, Phys. Rev. B **104**, 104305 (2021).

[47] L. Hackl, E. Bianchi, R. Modak, and M. Rigol, Entanglement production in bosonic systems: Linear and logarithmic growth, Phys. Rev. A **97**, 032321 (2018).

[48] G. Lindblad, On the generators of quantum dynamical semigroups, Commun. Math. Phys. **48**, 119 (1976).

[49] V. Gorini, A. Kossakowski, and E. C. G. Sudarshan, Completely positive dynamical semigroups of N-level systems, J. Math. Phys. **17**, 821 (1976).

[50] A. Metelmann and A. A. Clerk, Nonreciprocal photon transmission and amplification via reservoir engineering, Phys. Rev. X **5**, 021025 (2015).

[51] M. Tsang and C. M. Caves, Evading quantum mechanics: Engineering a classical subsystem within a quantum environment, Phys. Rev. X **2**, 031016 (2012).

[52] C. B. Møller, R. A. Thomas, G. Vasilakis, E. Zeuthen, Y. Tsaturyan, M. Balabas, K. Jensen, A. Schliesser, K. Hammerer, and E. S. Polzik, Quantum back-action-evading measurement of motion in a negative mass reference frame, Nature (London) **547**, 191 (2017).

[53] Note that at the QMFS point, we only need two auxiliary register modes to fully capture long-time conditional entanglement generation using a protocol that is similar to Eq. (3) but with different time-modulating functions $f_j(t;t_f)$.

[54] T. Holstein and H. Primakoff, Field dependence of the intrinsic domain magnetization of a ferromagnet, Phys. Rev. **58**, 1098 (1940).

[55] J. A. Hines, S. V. Rajagopal, G. L. Moreau, M. D. Wahrman, N. A. Lewis, O. Marković, and M. Schleier-Smith, Spin squeezing by Rydberg dressing in an array of atomic ensembles, Phys. Rev. Lett. **131**, 063401 (2023).

[56] E. S. Cooper, P. Kunkel, A. Periwal, and M. Schleier-Smith, Graph states of atomic ensembles engineered by photon-mediated entanglement, Nat. Phys. **20**, 770 (2024).

[57] This is similar to the situation of going from Clifford to non-Clifford circuits.

[58] J. Rieser, M. A. Ciampini, H. Rudolph, N. Kiesel, K. Hornberger, B. A. Stickler, M. Aspelmeyer, and U. Delić, Tunable light-induced dipole-dipole interaction between optically levitated nanoparticles, Science **377**, 987 (2022).

[59] J. F. Poyatos, J. I. Cirac, and P. Zoller, Quantum reservoir engineering with laser cooled trapped ions, Phys. Rev. Lett. **77**, 4728 (1996).

[60] P. M. Harrington, E. J. Mueller, and K. W. Murch, Engineered dissipation for quantum information science, Nat. Rev. Phys. **4**, 660 (2022).

[61] H. Krauter, C. A. Muschik, K. Jensen, W. Wasilewski, J. M. Petersen, J. I. Cirac, and E. S. Polzik, Entanglement generated by dissipation and steady state entanglement of two macroscopic objects, Phys. Rev. Lett. **107**, 080503 (2011).

[62] D. Kienzler, H.-Y. Lo, B. Keitch, L. de Clercq, F. Leupold, F. Lindenfelser, M. Marinelli, V. Negnevitsky, and J. P. Home, Quantum harmonic oscillator state synthesis by reservoir engineering, Science **347**, 53 (2015).

[63] C. Flühmann, T. L. Nguyen, M. Marinelli, V. Negnevitsky, K. Mehta, and J. P. Home, Encoding a qubit in a trapped-ion mechanical oscillator, Nature (London) **566**, 513 (2019).

[64] E. E. Wollman, C. U. Lei, A. J. Weinstein, J. Suh, A. Kronwald, F. Marquardt, A. A. Clerk, and K. C. Schwab, Quantum squeezing of motion in a mechanical resonator, Science **349**, 952 (2015).

[65] J.-M. Pirkkalainen, E. Damskägg, M. Brandt, F. Massel, and M. A. Sillanpää, Squeezing of quantum noise of motion in a micromechanical resonator, Phys. Rev. Lett. **115**, 243601 (2015).

[66] C. U. Lei, A. J. Weinstein, J. Suh, E. E. Wollman, A. Kronwald, F. Marquardt, A. A. Clerk, and K. C. Schwab, Quantum nondemolition measurement of a quantum squeezed state beyond the 3 dB limit, Phys. Rev. Lett. **117**, 100801 (2016).

[67] L. Piroli, G. Styliaris, and J. I. Cirac, Quantum circuits assisted by local operations and classical communication: Transformations and phases of matter, Phys. Rev. Lett. **127**, 220503 (2021).

[68] N. Tantivasadakarn, A. Vishwanath, and R. Verresen, Hierarchy of topological order from finite-depth unitaries, measurement, and feedforward, PRX Quantum **4**, 020339 (2023).

[69] E. Bäumer, V. Tripathi, D. S. Wang, P. Rall, E. H. Chen, S. Majumder, A. Seif, and Z. K. Minev, Efficient long-range entanglement using dynamic circuits, PRX Quantum **5**, 030339 (2024).

[70] A. Seif, Y.-X. Wang, and A. A. Clerk, Distinguishing between quantum and classical markovian dephasing dissipation, Phys. Rev. Lett. **128**, 070402 (2022).

[71] K. Jacobs and D. A. Steck, A straightforward introduction to continuous quantum measurement, Contemp. Phys. **47**, 279 (2006).

[72] J. Eisert, S. Scheel, and M. B. Plenio, Distilling Gaussian states with Gaussian operations is impossible, Phys. Rev. Lett. **89**, 137903 (2002).

[73] J. Fiurášek and L. Mišta, Gaussian localizable entanglement, Phys. Rev. A **75**, 060302(R) (2007).

[74] C. A. Regal, J. D. Teufel, and K. W. Lehnert, Measuring nanomechanical motion with a microwave cavity interferometer, Nat. Phys. **4**, 555 (2008).

[75] N. C. Menicucci, S. T. Flammia, and P. van Loock, Graphical calculus for Gaussian pure states, Phys. Rev. A **83**, 042335 (2011).

[76] J. T. Barreiro, M. Müller, P. Schindler, D. Nigg, T. Monz, M. Chwalla, M. Hennrich, C. F. Roos, P. Zoller, and R. Blatt, An open-system quantum simulator with trapped ions, Nature (London) **470**, 486 (2011).